Physics Letters B 809 (2020) 135762

Contents lists available at ScienceDirect

Physics Letters B

www.elsevier.com/locate/physletb

Observation of the 0_2^+ and γ bands in ^{98}Ru, and shape coexistence in the Ru isotopes

P.E. Garrett [a,b,*], L. Makhathini [c,d], R.A. Bark [c], T.R. Rodríguez [e], S. Valbuena [a], V. Bildstein [a], T.D. Bucher [c,d], C. Burbadge [a], R. Dubey [b], T. Faestermann [f], R. Hertenberger [g], M. Kamil [b], E.A. Lawrie [b,c], K.G. Leach [h], A.D. MacLean [a], C. Mehl [b], S.H. Mthembu [c,i], N.J. Mukwevho [b], C. Ngwetsheni [b], S.S. Ntshangase [i], J.C. Nzobadila Ondze [b], J.N. Orce [b], B. Rebeiro [b], B. Singh [b], S. Triambak [b], E.C. Vyfers [b], H.-F. Wirth [g]

[a] Department of Physics, University of Guelph, Guelph, ON, N1G2W1 Canada
[b] Department of Physics and Astronomy, University of the Western Cape, P/B X17, Bellville ZA-7535, South Africa
[c] iThemba LABS, National Research Foundation, P.O. Box 722, Somerset West 7129, South Africa
[d] Department of Physics, Stellenbosch University, Private Bag X1, Matieland 7602, South Africa
[e] Departamento de Física Teórica and CIAFF, Universidad Autónoma de Madrid, E-28049 Madrid, Spain
[f] Physik Department, Technische Universität München, D-85748 Garching, Germany
[g] Fakultät für Physik, Ludwig-Maximilians-Universität München, D-85748 Garching, Germany
[h] Department of Physics, Colorado School of Mines, 1523 Illinois St., Golden, CO 80401, USA
[i] Department of Physics, University of Zululand, KwaDlangezwa 3886, South Africa

ARTICLE INFO

Article history:
Received 1 May 2020
Received in revised form 31 July 2020
Accepted 1 September 2020
Available online 4 September 2020
Editor: Betram Blank

ABSTRACT

Excited states in ^{98}Ru were investigated using γ-ray spectroscopy following the β-decay of ^{98}Rh, and via the ^{100}Ru(p,t) reaction. Combining the results from the two experiments, two states were revised to have spin-parity of 4^+ and subsequently assigned to the 0_2^+ and "γ" bands, respectively. The observed structures in ^{98}Ru are suggested to be deformed and rotational, rather than spherical and vibrational, and fit well into the systematics of these excitations in the Ru isotopes. The 0_2^+ excitation is suggested as a shape coexisting configuration. This observation eliminates some of the last remaining candidates for nearly harmonic vibrational nuclei in the $Z \approx 50$ region. Beyond-mean-field calculations are presented that support shape coexistence throughout the Ru isotopes with $N = 52$–62, and suggest a smooth evolution of the shapes.

1. Introduction

The Ru isotopes are in a region where an abundance of examples of shape coexistence exists. With $Z = 44$, they are located midway between the Sr/Zr isotopes, for which the most rapid change in ground state shape across the nuclear chart is observed between $N = 58$ and $N = 60$, and the Cd/Sn isotopes that may be considered as iconic examples of nuclei possessing shape coexistence (for a review of shape coexistence, see, e.g. Ref. [1]). Sudden shape changes may be interpreted as a result of an inversion of two distinct configurations associated with unique nuclear deformations. Indeed, the shape transition at $N = 60$ in the Zr and Sr isotopes is accompanied by the appearance of low-lying 0_2^+ states indicating possible shape coexistence [1] and, similar to the 2_1^+ state, an abrupt drop of the 0_2^+ energy is observed at $N = 60$. The recent Coulomb excitation study of ^{96,98}Sr [2,3] provided firm evidence for configuration inversion in these nuclei, demonstrating important similarities in terms of transition probabilities and spectroscopic quadrupole moments between the ground-state band in ^{96}Sr and the structure built on the 0_2^+ state in ^{98}Sr. The local character of the shape change suggests that specific proton and neutron orbitals are responsible for this effect. Recent advances with the Monte Carlo shell model (MCSM) have made it possible to investigate the origin of the shape transition at $N = 60$ [4] and relate it to the strong proton-neutron interaction between proton $1g_{9/2}$ and neutron $1g_{7/2}$ sub-shells, and with the filling of the $1g_{7/2}$ neutron orbital, multi-particle excitations across the $Z = 40$ sub-shell gap becoming energetically more favourable inducing collectivity and deformation. The self-reinforcing effect, known as type-II shell evolution [5], is suggested to be responsible for the appearance of deformed states in Zr isotopes. Because these specific particle-

* Corresponding author.
E-mail address: pgarrett@physics.uoguelph.ca (P.E. Garrett).

https://doi.org/10.1016/j.physletb.2020.135762

hole excitations lead to a significant reorganization of the effective single-particle energies, the mixing of normal states and those with deformation-optimized shell structure is suppressed, consistent with experimental results.

As we move away from the Sr/Zr isotopes towards those with higher Z, the rapid change in the energies of the 2_1^+ and 0_2^+ states becomes far more gradual. In the Mo isotopes ($Z = 42$), detailed Coulomb excitation studies of ^{98}Mo [6] indicated that the 0_2^+ state, which appears *below* the 2_1^+ level, was deformed and prolate in shape. Further Coulomb excitation studies [7] of ^{100}Mo confirmed this picture, and provided strong evidence of shape coexistence in the Mo isotopes. The measured quadrupole moment [6] of the 2_1^+ state in ^{98}Mo indicates that it has either a spherical or completely γ-soft shape, in contrast to the prolate nature of the 0_2^+ state. The picture of shape coexistence is confirmed by large values of $\rho^2(E0; 0_2^+ \rightarrow 0_1^+)$ observed in ^{98,100,102}Mo [8], indicating both a change in $\langle\beta^2\rangle$, where β is the deformation parameter, and mixing of the configurations.

The Ru isotopes with neutron number $N \geq 60$ behave as deformed rotational nuclei. The Coulomb excitation study of ^{104}Ru performed by Srebrny et al. [9] provided a large set of matrix elements that enabled rather precise determinations of the invariant quantities $\langle Q^2\rangle$ and $\langle Q^3 \cos 3\delta\rangle$ (see Ref. [10] for their definition). For the ground-state band, the values are approximately constant up to the 8_1^+ level with $\langle Q^2\rangle \approx 0.9\ e^2b^2$, corresponding to $\beta_2 \approx 0.28$, and the variance extracted [9] was $\sigma(Q^2) \approx 0.22(6)$, indicating some dispersion in $\langle Q^2\rangle$ but with definite static deformation. The value of $\langle\cos 3\delta\rangle$ for the ground-state band corresponds to a triaxial shape with $\gamma \approx 25°$ [9]. For the 0_2^+ level, $\langle Q^2\rangle = 0.52(12)\ e^2b^2$ ($\beta_2 \approx 0.21$), indicating substantially smaller deformation, and $\langle\cos 3\delta\rangle = 0.1(3)$ [9] corresponding to $\gamma = 28(6)°$.

The structures of the Ru isotopes with $N < 58$ have often been discussed in terms of spherical vibrational motion. The proximity in energy of the 0_2^+, 2_2^+, and 4_1^+ states in ^{98,100,102}Ru, at approximately twice the energy of the 2_1^+ level, is suggestive of a spherical vibrator. Indeed, this was the main criteria used in a survey by Kern et al. [11] seeking examples of $U(5)$ nuclei. A recent update, using an expanded set of criteria [12], of the previous survey [11] found that few candidates remained. In fact, it was only ^{98,100}Ru that might be considered as possible spherical vibrational nuclei up to the excitation energy scale of the two-phonon states. Recent investigations of the structure of ^{98,100}Ru have considered interpretations around this central theme. Konstantinopoulos et al. [13] considered ^{100}Ru as a possible $E(5)$ [14] candidate, based on the yrast-band energies, but the $B(E2)$ values did not display the increasing trend predicted. The structure of ^{98}Ru was investigated by Cakirli et al. [15] using the ^{96}Mo$(\alpha, 2n)$ reaction, and concluded that the possible candidates for the three-phonon states could not be described with an anharmonic vibrator description, and further that *none* of the higher-lying states in ^{98}Ru bore any resemblance to three-phonon states. Thus, if ^{98}Ru were vibrational, the vibrational pattern appeared to terminate at the two-phonon level [15].

The most recent experimental study [16–18] of ^{98}Ru utilized the ^{97}Mo(^{3}He,2n) reaction and observed states up to spin 10. The spin-parities of levels were deduced through a combination of conversion electron, γ-ray angular distributions, and γ-γ angular correlations. A number of additional levels were observed, as well as transitions amongst previously known states. Some key points on the level scheme are noted. For the level at 1817 keV, Cakirli et al. [15] considered possible spin values of 0^+ and 2^+, since they considered the existence of the 1817 keV γ-ray transition to the ground state as tentative only. Giannatiempo et al. [17], on the other hand, observed this transition and proposed a spin-parity of 2^+. The 1817 keV level is fed by a 610 keV γ-ray transition from a level at 2428 keV, assigned by both Cakirli et al. [15] and Giannatiempo et al. [17] as a 2^+ state. A level at 2013 keV had a firm assignment of $I^\pi = 3^+$ in these studies [15,17] that was adopted from earlier works as summarized in Ref. [19]. As will be shown below, these states are key to unravelling the structure of ^{98}Ru.

2. Experimental details and results

The use of γ-ray spectroscopy following β-decay has proven to be a highly sensitive technique for the observation of non-yrast levels and weak decay branches, and it was employed here to study ^{98}Ru. The ^{98}Rh parent has two β-decaying states: the ground state with $J^\pi = (2)^+$, Q-value of $Q = 5057(10)$ keV, $t_{1/2} = 8.72(12)$ min, and an excited state with $J^\pi = (5^+)$ and $t_{1/2} = 3.6(2)$ min with a β^+/EC branching ratio of $11 \pm 5\%$ [19]. The presence of the two β-decaying states in ^{98}Rh, with the large spin difference, provided the opportunity to observe a range of spins up to $6\hbar$ in the daughter nucleus ^{98}Ru.

The present results represent the first experiment using the newly commissioned iThemba LABS Tape Station. The ^{98}Rh activity was produced by using the ^{89}Y(^{12}C,3n)^{98}Rh reaction. Beams of 47.5 MeV ^{12}C ions, obtained from the iThemba LABS K200 cyclotron, with currents up to 8 pnA bombarded a ^{89}Y foil of thickness 250 μm obtained from Goodfellow Inc. The ^{89}Y foil was mounted on a wagon that was attached to the tape in the center of the target chamber. The irradiation period was chosen to be 18 minutes, or approximately 2 half lives of the ground state activity, following which the beam was stopped and the tape was moved. After a transit of approximately 2 minutes, the wagon was stopped immediately in front of a NE102 plastic scintillator of dimension 40×45 mm and 5 mm thickness coupled to a photomultiplier tube. A 5 mm thick Si(Li) detector could be introduced into the counting chamber via a gate valve and positioned geometrically opposite of the plastic scintillator in direct view of the beam-irradiated side of the target foil, and used for conversion electron detection. Positioned exterior to the counting chamber were three unsegmented AFRODITE HPGe clover detectors and one segmented HPGe clover of the TIGRESS design [20]. The HPGe detectors were equipped with bismuth germanate (BGO) Compton-suppression shields. All signals were processed with the PIXE Digital Gamma Finder (DGF) modules, and readout achieved with the aid of the MIDAS data acquisition system [21] operating in a triggerless acquisition mode. The decay activity was measured for 18 minutes, following which the wagon was transported back to the target chamber and the cycle repeated. During the course of the measurement, approximately 120 of the 40-minute irradiation-counting cycles were completed.

Approximately 1×10^9 BGO-suppressed events were registered by the HPGe detectors after applying the addback condition. Of these, 230×10^6 events were also in coincidence with the plastic scintillator, which selects the β^+ decay branch only. The β^+-particle tagging on the γ-γ matrix was deemed unnecessary since the source activity was well above room background, and thus the analysis was performed on the time-random-background subtracted γ-γ matrix that contained 25×10^6 events.

Shown in the top panel of Fig. 1 is a portion of the spectrum of γ rays in coincidence with the 762-keV $2_2^+ \rightarrow 2_1^+$ γ ray, showing clearly the presence of a newly observed 403-keV γ-ray decay of the 1817-keV level. Its placement is shown in the partial level scheme in Fig. 2. With the observation of the γ-ray transitions to the $0_{1,2}^+$ and 4_1^+ levels, the spin-parity of the 1817-keV state assigned in Ref. [17] as the 2_3^+ level is confirmed. A new 216-keV γ-ray decay from the 2013-keV level, previously assigned as the 3_2^+ state, to the 1797-keV 3_1^+ state is also observed. These and other relevant results are summarized in Table 1.

The β-decay experiment was complemented with the ^{100}Ru$(p, t)^{98}$Ru reaction performed at the Maier-Leibnitz Labora-

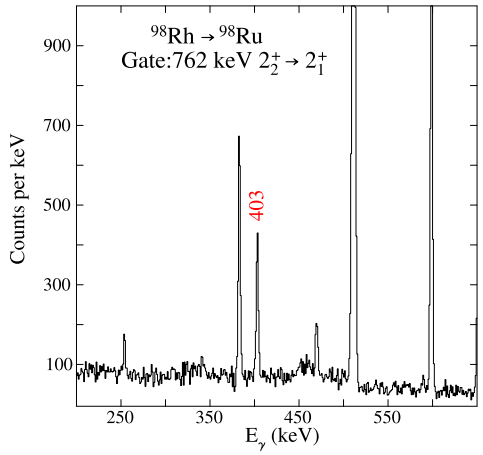

Fig. 1. Portion of the spectrum of γ rays observed in the β^+/EC decay of ^{98}Rh, created with a coincidence condition with the 762 keV $2_2^+ \rightarrow 2_1^+$ transition. The newly-observed 403 keV γ ray from the 2_3^+ level is indicated.

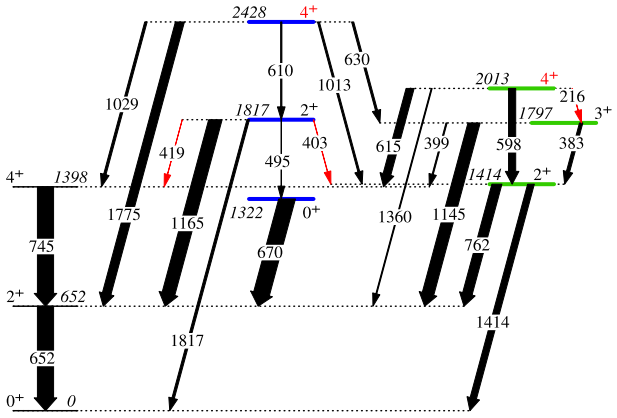

Fig. 2. Partial level scheme of ^{98}Ru displaying the 0_2^+ and γ bands assigned in the present work. New information is highlighted in red. The transitions are labelled with their energies in keV, and the widths of the arrows are proportional to the measured branching ratios. The spins of the 2013- and 2428-keV levels were determined in the ^{100}Ru(p,t) two-neutron-transfer reaction.

Table 1
Results for the levels assigned to the 0^+ and γ-band in ^{98}Ru obtained from the β^+/EC decay of ^{98}Rh. The initial (E_i) and final (E_f) level energies are given in keV. The uncertainties on the γ-ray transition energies, E_γ, include a systematic uncertainty of 0.05 keV, and a 5% systematic uncertainty is included on the γ-ray intensities used to determine the branching fractions.

E_i	I_i^π	E_γ	E_f	I_f^π	Branching
1414.3	2^+	761.76(11)	652.4	2^+	0.396(14)
		1414.46(13)	0.0	0^+	0.604(14)
1797.0	3^+	382.66(11)	1414.3	2^+	0.196(11)
		398.95(12)	1397.8	4^+	0.071(5)
		1144.51(11)	652.4	2^+	0.733(14)
2012.7	4^+	215.68(8)	1797.0	3^+	0.019(2)
		598.46(5)	1414.3	2^+	0.441(17)
		614.91(5)	1397.8	4^+	0.483(17)
		1360.3(2)	652.4	2^+	0.057(7)
1322.1	0^+	669.76(8)	652.4	2^+	1.0
1817.2	2^+	402.90(7)	1414.3	2^+	0.0220(15)
		419.17(11)	1397.8	4^+	0.0056(6)
		495.05(6)	1322.1	0^+	0.0152(11)
		1164.75(5)	652.4	2^+	0.762(12)
		1817.31(10)	0.0	0^+	0.196(11)
2427.6	4^+	610.34(24)	1817.2	2^+	0.075(9)
		629.82(11)	1797.0	3^+	0.126(11)
		1012.90(13)	1414.3	2^+	0.112(11)
		1029.65(8)	1397.8	4^+	0.144(13)
		1775.17(8)	652.4	2^+	0.541(20)

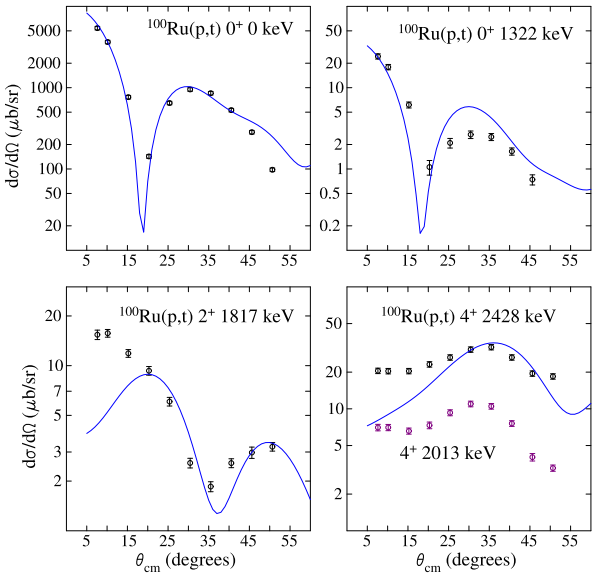

Fig. 3. Angular distributions observed in the ^{100}Ru$(p,t)^{98}$Ru reaction performed with 22 MeV proton beams. The curves are the result of FRESCO calculations for a di-neutron transfer.

tory [22]. Beams of 22 MeV protons up to 2 μA current bombarded a target of ^{100}Ru 110 μg/cm^2 thick, and the products of the reaction were momentum analyzed with the Q3D spectrograph. The (p,t) transfer data were collected at 10 angles from 7.5° to 50°, and elastic scattering data were collected in 5° intervals from 10° to 115° and used to determine the target thickness as well as the optimum choice of the proton optical-model potential.

Two-neutron-transfer reactions on $I^\pi = 0^+$ targets selectively populate natural parity states since the two neutrons are coupled to $S = 0$ and hence the final states have $I = L$, where L is the orbital angular momentum of the transfer, and parity $\pi = (-1)^L$. Fig. 3 displays angular distributions of some selected states observed in the ^{100}Ru$(p,t)^{98}$Ru reaction; the ground state, the 1322-keV 0_2^+ state, the 1817-keV 2^+ state, and the states at 2013 keV and 2428 keV. The previous spin-parity assignments for the 2013 keV and 2428 keV states were 3^+ and 2^+, respectively [17]. As can be seen in Fig. 3, the angular distribution of the 2428-keV level does not match that of the assigned 2^+ state at 1817 keV, but mirrors that of the 2013-keV level. A 3^+ state should not be populated strongly in the (p,t) reaction (the 1797 keV 3_1^+ level is not observed, for example), and thus a 3^+ assignment for the 2013-keV level can be immediately ruled out. Also shown on the plots in Fig. 3 are curves resulting from FRESCO [23] calculations for the $L = 0, 2, 4$ transfers to the respective states. These curves are calculated including only the single-step direct di-neutron transfer involving $g_{7/2}$ neutrons. The calculations are not intended to reproduce exactly the observed angular distributions, which would necessitate the use of more complicated wave functions and include multi-step processes including sequential transfer, but do display an overall qualitative agreement with the data. From these data, the 2013-keV and 2428-keV levels are firmly assigned as $I^\pi = 4^+$.

With the new spin assignments, the level scheme displayed in Fig. 2 strongly suggests the presence of a band based on the 0_2^+ level at 1322 keV, and also a γ band based on the 2_2^+ level at 1414 keV. (We use the label "γ band" to indicate the $\Delta I = 1$ sequence built on the 2^+ state, irrespective of its underlying character.) The key to these suggested bands are the re-assignments of the spins of the 2428-keV and 2013-keV levels to 4^+. Shown in Fig. 4 are the systematics of the 0_1^+, 0_2^+, and γ bands in $^{96-106}$Ru, and it can be seen that the newly assigned band structures in ^{98}Ru fit the

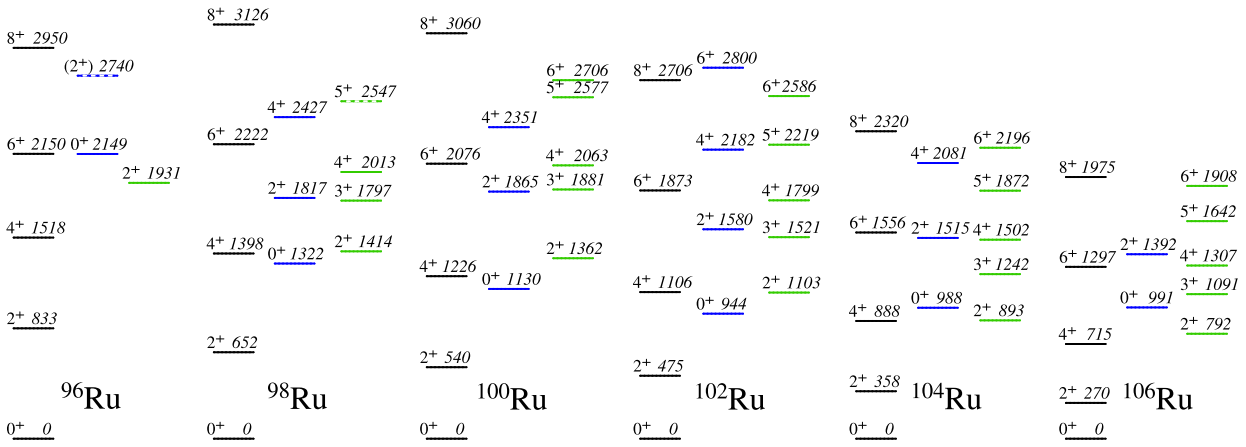

Fig. 4. Partial level schemes of the Ru isotopes from $A = 96$ to $A = 106$ displaying the ground-state bands, 0_2^+ bands, and γ bands observed experimentally, extracted from Ref. [24] and the results of the present work. The levels are labelled with their energies in keV.

systematics well. The γ bands display a very smooth evolution as a function of neutron number, with the maximal staggering observed in ^{100}Ru [25]. The 5_1^+ state in ^{98}Ru was too weakly populated in the present experiment to permit observation of its in-band decay, and thus its assignment is based only on the energy systematics.

3. Theoretical calculations and discussion

3.1. The ground state, γ, and 0_2^+ bands

The present results are discussed in terms of intrinsic shapes calculated within the symmetry conserving configuration mixing framework (SCCM) using the Gogny D1S as the underlying nuclear interaction [26]. This is a fully microscopic method based on an extension of the mean-field approximation that includes particle number and angular momentum projections of Hartree-Fock-Bogoliubov (HFB) states defined along the intrinsic quadrupole degrees of freedom, (β_2, γ). The final nuclear wave functions are obtained as linear combinations of these symmetry-restored states whose coefficients are found within the generator coordinate method. In the present implementation, the HFB states are produced with the particle-number variation after projection method (PN-VAP) that ensures a better description of pairing correlations than the plain HFB method. In addition, parity and time-reversal symmetries are preserved by the HFB states, and only quasiparticle vacua are included in the definition of the SCCM wave functions. Hence, neither negative parity states are described nor an optimal variational exploration of the excited states is performed. Therefore, we provide a more qualitative than quantitative description of the structure of the nuclei studied here.

A common feature of the SCCM results for $^{96-106}$Ru isotopes is the grouping of the lowest excited states in three bands, namely, the ground state and second excited state bands built on top of 0^+ states with $\Delta I = 2$, and a first excited state band with $\Delta I = 1$ and a 2_γ^+ band-head corresponding to the "γ-bands" labelled above. In Fig. 5, we compare the experimental and theoretical excitation energies of the band-heads and the first members of those bands along the isotopic chain. For the ground-state and γ-bands the agreement is very good considering the limitations of the present SCCM implementation. Thus, the 2_1^+ and 4_1^+ energies decrease with increasing the number of neutrons because we are moving away from the $N = 50$ shell closure and an increase of the deformation, and, consequently, a more rotational behaviour is expected. In addition, the 2_γ^+ and 3_1^+ energies also decrease (with the exception for ^{100}Ru, that slightly increases) suggesting that these isotopes become triaxially deformed. This evolution is confirmed

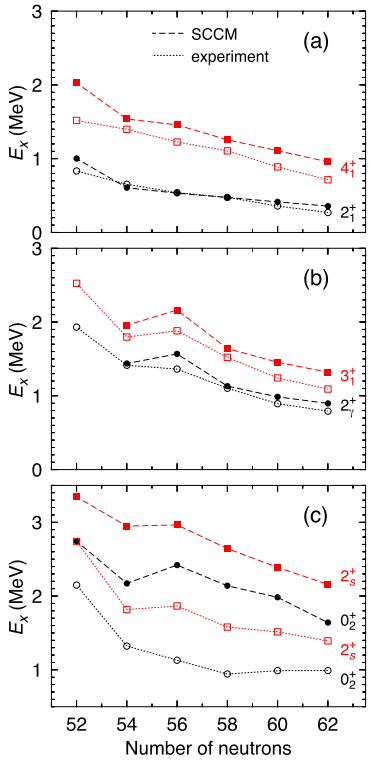

Fig. 5. Comparison of the experimentally observed energies (open points) and results of the SCCM calculations (filled points) for (a) the ground-state band, (b) the γ band, and (c) the 0_2^+ band.

by the analysis of the ground state and 2_γ^+ wave function distributions shown in Fig. 6. The (β_2, γ) deformation of the ground state wave functions changes from (0.15, 0°) for ^{96}Ru to (0.3, 20°) for ^{106}Ru. The wave function distributions for the 2_γ^+ state are peaked at $(\beta_2, \gamma) = (0.2, 35°)$ for ^{96}Ru, and evolve smoothly to larger deformation and smaller values of γ reaching (0.3, 20°) for ^{106}Ru, and bear a strong similarity to the distributions for the 0_1^+ states except for ^{96}Ru. None of the predicted distributions for the 2_γ^+ states resemble those for a two-phonon vibrational state, that would necessitate the presence of a clear node in the wave functions, and the presence of γ bands argues against a spherical interpretation for the ground states for the $N \geq 54$ Ru isotopes.

We also display in Fig. 5(c) the evolution of the energies of the 0_2^+ states and their corresponding 2_s^+ band members. We clearly see that the agreement is worse than in the two previous bands

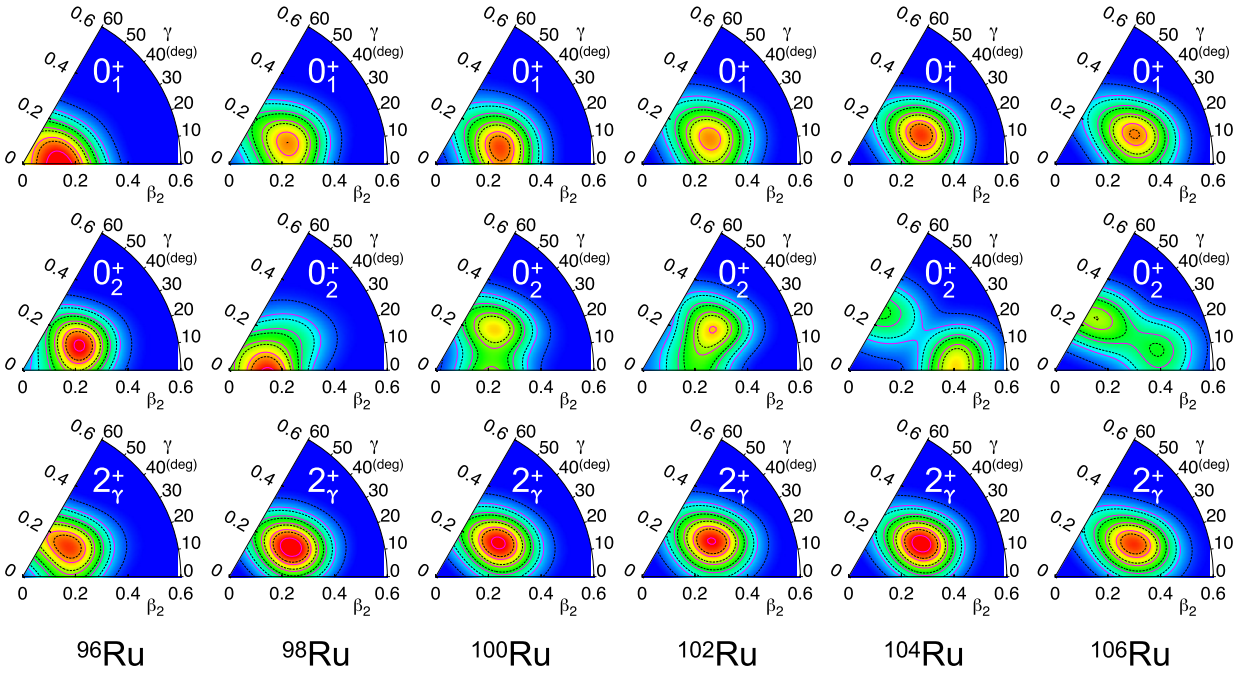

Fig. 6. Wave function distributions in the (β_2, γ) plane for the 0_1^+ (top), 0_2^+ (middle), and 2_γ^+ (bottom) states resulting from the SCCM calculations.

although the trend of the 2_s^+ is reproduced well. The evolution of the wave function distributions for the 0_2^+ states (see Fig. 6) for $^{96-106}$Ru is not as smooth as those of the ground-state and γ bands. Mainly triaxial configurations with different degrees of mixing (^{96,100,102}Ru), prolate (^{98}Ru), and with a large degree of mixing (^{104,106}Ru) of the shapes are found for the 0_2^+ states.

The 0_2^+ state in ^{104}Ru is known to be a shape-coexisting state, as was established from the Coulomb excitation results that yield $(\beta_2, \gamma) = (0.21, 28°)$ compared to the ground state with $(\beta_2, \gamma) = (0.28, 25°)$ [9]. Urban et al. [28] suggested there are two relatively unperturbed configurations for the 0^+ states at $N = 52$ which evolve differently with N (see Fig. 5 of Ref. [28]). The first configuration forms the ground state in ^{96}Ru that has a nearly spherical shape. The deformation of this configuration remains approximately constant with N and always small, and at $N = 60$ becomes the excited 0_2^+ band. The second configuration is the 0_2^+ state in ^{96}Ru, and also possesses low deformation, however it was suggested that its deformation increases with N. These two configurations cross in the vicinity of ^{100,102}Ru such that this deformed second configuration becomes the ground state band in ^{104}Ru. As a result of the mixing near the crossing, both 0^+ states take on deformed characteristics.

With the newly-established 0_2^+ band in ^{98}Ru, it is proposed to be deformed and rotational in character with a deformation greater than that of the ground state, as inferred from the level spacing. This larger deformation, however, is not reflected in the SCCM calculations, where the 0_2^+ wave function distribution has a maximum near $(\beta_2, \gamma) = (0.15, 0°)$, and that for 0_1^+ has $(\beta_2, \gamma) = (0.22, 25°)$. The SCCM calculations reflect a crossing occurring between $N = 52$ ^{96}Ru and $N = 54$ ^{98}Ru, but then the 0_2^+ state takes on a completely different character in ^{100}Ru, with $(\beta_2, \gamma) = (0.25, 45°)$. In order to test the proposition of a crossing between the 0_1^+ and 0_2^+ configurations, we performed two-state mixing calculations, to solve for the unmixed level energies, using the 400 keV matrix element proposed by Urban et al. [28]. The result of these calculations, which plot the excitation energy minus a rigid-rotor estimate, is shown in Fig. 7. The excited 0_2^+ band in ^{98}Ru has a larger moment of inertia than the ground state band, whereas

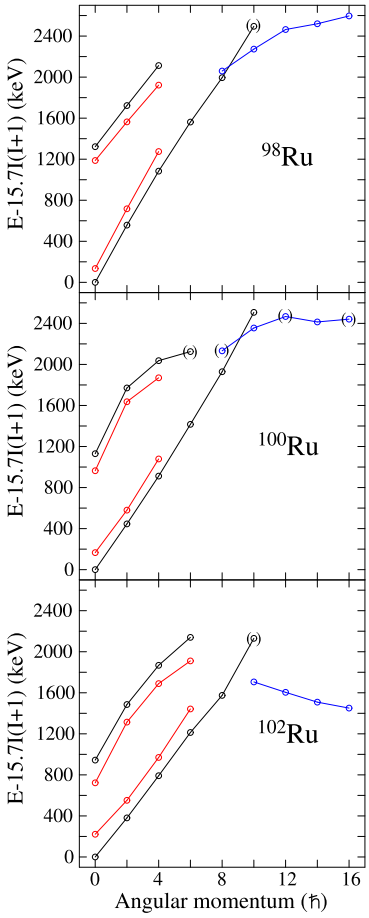

Fig. 7. Excitation energies minus the rigid-rotor estimates for the ground-state band, 0_2^+ band, and the high-spin yrast band (blue) for ^{98}Ru (top), ^{100}Ru (middle), and ^{102}Ru (bottom). Also shown are the estimated unperturbed energies of the 0_1^+ and 0_2^+ bands assuming two-state mixing with a constant 400 keV interaction (red). Data points within parentheses have tentative spin values.

the opposite is true in ^{100}Ru and ^{102}Ru, suggesting that the crossing of the configurations occurs between ^{98}Ru and ^{100}Ru. (The curvature observed for the higher-spin members of the 0_2^+ bands in ^{100,102}Ru likely reflects interactions with other configurations – in all three nuclei the ground state band is crossed with another configuration between spin 8 and 10.)

From an examination of the potential energy surfaces (PES), examples of which are shown in Fig. 5 of Ref. [25] for $^{98-104}$Ru, it is not evident that the calculations predict shape coexistence. The PES do not appear to exhibit two or more well-developed minima that would support the generation of states forming collective bands associated with their respective energy wells. However, the configuration mixing calculations show different bands built on collective wave functions that peak at significantly different deformations, and do not possess a clear nodal structure, specifically in $^{96-102}$Ru. These collective wave functions are rather extended in the (β_2, γ) plane, and the mixing of shapes is important. Thus, the manifestation of shape coexistence in the Ru isotopes is less evident than in, for example, the Cd isotopes [29,30].

Very recently, in an extended analysis of the systematics in the Sr–Sn region for neutron numbers 52–66, Urban et al. [31] advocated that $(2p2h)$ neutron intruder configurations, created by the promotion of neutrons from the $d_{5/2}$ to the $g_{7/2}$ or $h_{11/2}$ orbitals, were playing an important role in the collectivity of the excited 0^+ states. Rather than the well-known case of intruder states built on $\pi(2p2h)$ excitations, where a parabolic trend in the excitation energies is observed as a function of neutron number symmetric about the neutron mid-shell, in this case the parabolic trend is observed as a function of the proton number (see Figs. 4–6 of Ref. [31]). If this scenario is the case, it may be expected that the neutron configurations of the 0_2^+ state in ^{98}Ru are similar to those of the 0_2^+ states in ^{96}Mo and ^{94}Zr, and the main differences would reside in the occupation of protons in the $p_{1/2}$ and $g_{9/2}$ orbitals. In ^{96}Mo, results from Coulomb excitation [32] yield the invariant $\langle Q^2 \rangle = 0.286(7)\ e^2b^2$ and $\langle Q^2 \rangle = 0.069^{+0.008}_{-0.010}\ e^2b^2$ for the 0_1^+ and 0_2^+ states, respectively, indicating vastly different shapes for the ground state and 0_2^+ state, but with the 0_2^+ state very weakly deformed. This would appear to be in contradiction with the 0_2^+ state in ^{96}Mo as an intruder excitation. The present results for ^{98}Ru, and previous observations in ^{94}Zr [33], on the other hand, favour a substantially higher degree of deformation for the 0_2^+ state. Using the known $B(E2)$ values in ^{94}Zr [33–35], the invariants for the 0_1^+ and 0_2^+ states are $\langle Q^2 \rangle = 0.116(5)\ e^2b^2$ and $\langle Q^2 \rangle = 0.34(3)\ e^2b^2$, respectively.

Shown in Fig. 8 are the differences between the number of particles expected with a normal filling of the Hartree-Fock (HF) spherical orbitals, and the number of particles computed with the SCCM wave functions [27]. For the protons, four particles are expected in the HF $g_{9/2}$ orbital, and thus systematically for the 0_1^+ state a greater occupancy is calculated (between four and five). Progressively, increasing in neutron number from $N = 52$ ^{96}Ru to $N = 60$ ^{104}Ru, we observe that the number of holes in the pf orbitals increases monotonically for the ground state, and the number of particles in the $g_{9/2}$ and $d_{5/2}$ orbitals increases substantially. As can be seen from the wave function distributions for the 0_1^+ and 0_2^+ states in Fig. 6, there appears to be an interchange of these states between ^{96}Ru and ^{98}Ru; this is also reflected in the proton occupancies where the distribution for the 0_2^+ state in ^{96}Ru is very similar to that of the 0_1^+ state in ^{98}Ru, and *vice versa*. Experimentally, the interchange appears to be slightly delayed compared to this prediction occurring between ^{98}Ru and ^{100}Ru.

For the neutron occupancy, the situation also changes isotope-by-isotope, especially for $d_{5/2}$ and $g_{7/2}$ orbitals. For example, the $g_{7/2}$ orbital should have, in the spherical HF configuration, zero particles for $^{96-100}$Ru, two particles in ^{102}Ru and four particles in ^{104}Ru. The $g_{7/2}$ occupancy is already substantial for ^{98,100}Ru, essentially in line with expectations for ^{102}Ru, and slightly less than expected for ^{104}Ru.

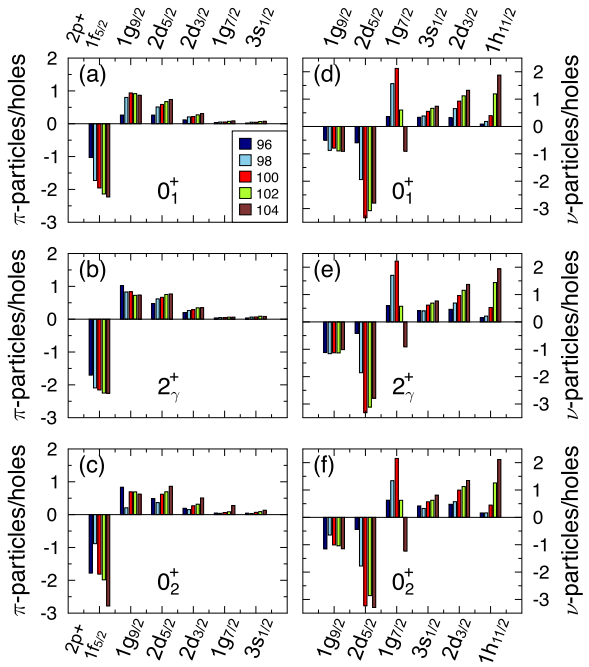

Fig. 8. Calculated occupancies of the orbitals near the Fermi surfaces in ^{96}Ru-^{104}Ru isotopes for the 0_1^+, 2_γ^+, and 0_2^+ states for protons (panels a) - c)) and neutrons (panels d) - f)), respectively. The height of the bars represents the *excess* of particles with respect to expected occupancies based on a spherical Hartree-Fock calculation, e.g. four protons in the $g_{9/2}$ orbital for the ground states.

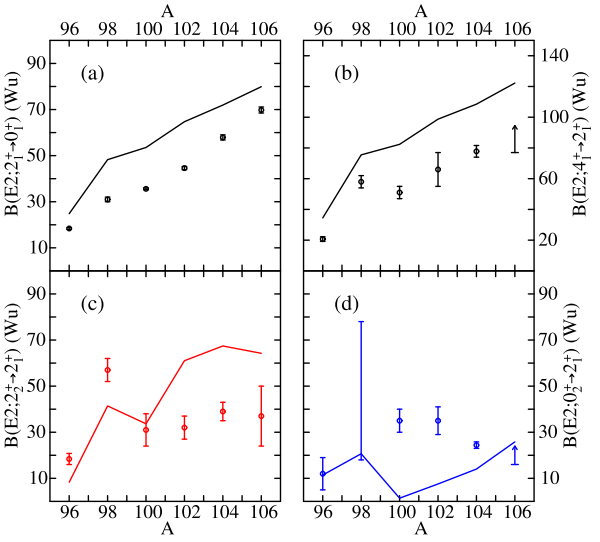

Fig. 9. $B(E2)$ values, in W.u., for the $2_1^+ \rightarrow 0_1^+$ (panel a), the $4_1^+ \rightarrow 2_1^+$ (panel b), the $2_2^+ \rightarrow 2_1^+$ (panel c) and the $0_2^+ \rightarrow 2_1^+$ (panel d) transitions. The data are taken from Ref. [24] except for ^{104}Ru, from Ref. [9], and ^{106}Ru from Ref. [36]. The $B(E2; 0_2^+ \rightarrow 2_1^+)$ value for ^{98}Ru has a wide range due to uncertainties in signs of matrix elements used in the analysis of the Coulomb excitation data [37]. Lower limits, due to upper limits on life times [36], are given for the $B(E2; 2_2^+ \rightarrow 2_1^+)$ and $B(E2; 0_2^+ \rightarrow 2_1^+)$ values for ^{106}Ru. The curves are the results of the SCCM calculations.

3.2. $B(E2)$ values

In Fig. 9 the calculated $B(E2)$ values for selected transitions from the first four excited states are shown. The transition

strengths in the yrast band are over-predicted, perhaps reflecting that the deformation is predicted to be too large. We note that even in ^{102}Ru, for which the calculated quadrupole moment reproduces the experimental value extremely well, the calculated $B(E2; 2_1^+ \rightarrow 0_1^+)$ value is approximately 45% too large. The $B(E2)$ values for the decay of the 2_2^+, the γ-band head, are under-predicted for ^{96,98}Ru, and over-predicted for $A > 100$, and that for decay of the 0_2^+ state are generally under-predicted, except for ^{96}Ru, and possibly ^{106}Ru for which only a lower limit is known.

Of interest is the trend, in both the calculations and the data, of the local peaking observed in some of the $B(E2)$ values that occurs at $A = 98$, and the dip at $A = 100$. In the calculations, the increases of the $B(E2; 2_1^+ \rightarrow 0_1^+)$, $B(E2; 4_1^+ \rightarrow 2_1^+)$, and $B(E2; 2_2^+ \rightarrow 2_1^+)$ values from ^{96}Ru to ^{98}Ru are due to the increase in deformation and the large overlap of the collective wave functions of the states involved in the transitions. The calculations further predict, from ^{98}Ru to ^{100}Ru, a slight increase of the $B(E2; 2_1^+ \rightarrow 0_1^+)$ and $B(E2; 4_1^+ \rightarrow 2_1^+)$ values (the latter is contrary to the experimental data) and a decrease of the $B(E2; 2_2^+ \rightarrow 2_1^+)$ value (in agreement with the data). In ^{100}Ru, the 2_1^+ state has a slightly greater axial deformation, and also possesses a slightly larger deformation than the corresponding state in ^{98}Ru, and the overlaps between the 4_1^+, 2_1^+, and 0_1^+ collective wave functions are large, while the overlap of the 2_2^+, which possesses a higher degree of triaxiality, and the 2_1^+ collective wave function become smaller.

4. Conclusions

The excited states of ^{98}Ru were investigated using γ-ray spectroscopy following the β decay of ^{98}Rh. The source activity was produced using the ^{12}C+^{89}Y reaction at the iThemba LABS Tape Station, and the present work represents the first results from this new facility. The β-decay data were complemented with results from the ^{100}Ru(p, t) reaction performed using 22 MeV proton beams at the Maier-Leibnitz Laboratory, with the reaction products analyzed with the Q3D magnetic spectrograph. The combination of data – additional γ-ray transitions and spin-parity assignments from the (p, t) angular distributions – permit the assignment of states to the γ and 0_2^+ bands.

The present work was motivated by a review [12] of purported spherical vibrational (or $U(5)$) states in the $Z = 40 - 50$ mass region where it was claimed that the current status of the experimental data could not rule out a multiphonon vibrational interpretation of the low-lying states in ^{98,100}Ru. The reassignment of the spins of the 2013- and 2428-keV states as 4^+, and the assignment of the 0_2^+ and the 2_γ^+ bands proves experimentally that the most plausible structure of ^{98}Ru assumes the existence of deformed bands. This is in contradiction to the spherical vibrational interpretation of the spectrum. These deformed collective bands are also predicted by the SCCM calculations where the spherical vibrational band is not present, making a strong argument against this latter interpretation. The newly assigned γ and 0_2^+ bands in ^{98}Ru have been shown to fit very well in the systematics of these excitations assigned in the heavier Ru isotopes, and the SCCM calculations predict that the $^{98-106}$Ru isotopes are deformed. We thus exclude the last remaining candidates [11,12] for nuclei possessing multiphonon spherical vibrational motion in the $Z = 40 - 50$ region – a region once believed to be rich in such structures. The differences observed in the energy spacings within the 0^+ bands are suggestive of structures possessing different deformations, and the SCCM calculations also indicate that the 0^+ bands have collective wave functions resulting in significant differences in the (β_2, γ) deformation parameters.

In order to test the trends predicted, and firmly establish the degree of deformation that the states possess, detailed Coulomb excitation measurements like those performed for ^{104}Ru [9] are required. Investigations along these lines have been initiated, with the first proposed experiments using the Coulomb excitation of ^{100}Ru with ^{14}N and ^{32}S beams approved at the Heavy-Ion Laboratory in Warsaw, and multi-step Coulomb excitation of ^{102}Ru at iThemba LABS in Cape Town.

Declaration of competing interest

The authors declare that they have no known competing financial interests or personal relationships that could have appeared to influence the work reported in this paper.

Acknowledgements

This work was supported in part by the Natural Sciences and Engineering Research Council (Canada). T.R.R. acknowledges computing time at GSI-Darmstadt and support from Spanish MICINN under PGC2018-094583-B-I00. We thank the iThemba LABS accelerator and instrumentation departments for their support.

References

[1] K. Heyde, J.L. Wood, Rev. Mod. Phys. 83 (2011) 1467.
[2] E. Clément, et al., Phys. Rev. Lett. 116 (2016) 022701.
[3] E. Clément, et al., Phys. Rev. C 94 (2016) 054326.
[4] T. Togashi, et al., Phys. Rev. Lett. 117 (2016) 172502.
[5] T. Otsuka, Y. Tsunoda, J. Phys. G, Nucl. Part. Phys. 43 (2016) 024009.
[6] M. Zielińska, et al., Nucl. Phys. A 712 (2002) 3.
[7] K. Wrzosek-Lipska, et al., Phys. Rev. C 86 (2012) 064305.
[8] J.L. Wood, et al., Nucl. Phys. A 651 (1999) 323.
[9] J. Srebrny, et al., Nucl. Phys. A 766 (2006) 25.
[10] D. Cline, Annu. Rev. Nucl. Part. Sci. 36 (1986) 683.
[11] J. Kern, et al., Nucl. Phys. A 593 (1995) 21.
[12] P.E. Garrett, et al., Phys. Scr. 93 (2018) 063001.
[13] T. Konstantinopoulos, et al., Phys. Rev. C 95 (2017) 014309.
[14] F. Iachello, Phys. Rev. Lett. 85 (2000) 3580.
[15] R.B. Cakirli, et al., Phys. Rev. C 70 (2004) 044312.
[16] A. Nannini, et al., Eur. Phys. J. Web Conf. 66 (2014) 02071.
[17] A. Giannatiempo, et al., Phys. Rev. C 94 (2016) 054327.
[18] A. Giannatiempo, Phys. Rev. C 96 (2017) 044326.
[19] B. Singh, Z. Hu, Nucl. Data Sheets 98 (2003) 335.
[20] H.C. Scraggs, et al., Nucl. Instrum. Methods A 543 (2005) 431.
[21] Software repository located at http://npg.dl.ac.uk/MIDAS/.
[22] G. Dollinger, T. Faestermann, Nucl. Phys. News Int. 28 (2018) 5.
[23] I.J. Thompson, Comput. Phys. Rep. 7 (1988) 167.
[24] Data extracted from the National Nuclear Data Center, www.nndc.bnl.gov.
[25] P.E. Garrett, et al., Acta Phys. Pol. B 51 (2020) 799.
[26] T.R. Rodríguez, J.L. Egido, Phys. Rev. C 81 (2010) 064323.
[27] T.R. Rodríguez, et al., Phys. Rev. C 93 (2016) 054316.
[28] W. Urban, et al., Phys. Rev. C 87 (2013) 031304(R).
[29] P.E. Garrett, et al., Phys. Rev. Lett. 123 (2019) 142502.
[30] P.E. Garrett, et al., Phys. Rev. C 101 (2020) 044302.
[31] W. Urban, et al., Phys. Rev. C 99 (2019) 064325.
[32] M. Zielińska, Ph.D. thesis, University of Warsaw (2005) (unpublished).
[33] A. Chakraborty, et al., Phys. Rev. Lett. 110 (2013) 022504.
[34] E. Elhami, et al., Phys. Rev. C 75 (2013) 011301(R); erratum Phys. Rev. C 88 (2013) 029902.
[35] E.E. Peters, et al., Phys. Rev. C 88 (2013) 024317.
[36] M. Sanchez-Vega, et al., Eur. Phys. J. A 35 (2008) 159.
[37] E. Williams, et al., Phys. Rev. C 74 (2006) 024302.